 CMES, vol.93, no.3, pp.221-234, 2013

Numerical Analysis on Dual Holes Interactions

C. K. Chen[1]

Abstract: By extending Bückner's superposition principle and alternating iteration method, this presentation studies the dual holes interactions. A newly developed numerical scheme is embedded in the conventional Gauss-Legendre quadrature routine for evaluating the boundary integral holding stress singularities. This developed scheme can avoid numerical singularity and facilitate the achieved stress field to be exact as that of analytical solution; however the chosen Gaussian integration points must enter a large quantity. This presentation uses an infinite plate with a centered hole strained by remote axial loading as a testing example, and the numerical results are capable of reaching the analytical solution in the evaluation. The accurate stress estimation in the stress field of the dual holes interacting can therefore locate the dual holes in a very close proximity and no divergence will occur during evaluating the interacting stress concentration between holes.

Keywords: Holes interactions, Alternating iteration, Bückner's superposition, Gauss-Legendre quadrature

1 Introduction

The local geometrical discontinuities, such as holes, notches, cracks etc., in the structures play important roles for engineering design. It is well-known that holes act as stress raisers, and therefore single hole stress concentration had been widely studied for various holes shapes in last several decades; please refer to the studies of Inglish (1913), Savin (1961), Muskhelishivili (1953) and Sokolnikoff (1956). Accurate prediction of explicit fracture would demand precise estimation on the growth of these stress raisers and their mutual interactions. Afterwards, interactions among cracks had been explored extensively. Many novel physical mathematics methods have thus been proposed to manipulate the elastic problems in multiple-connected region, namely Horri and Nemat-Nasser (1987) submitted superposition and pseudo-traction, Nisitani developed body force formulation and Chen (1997) also used superposition principles and body force doublets to deal with the crack

[1] Cheng Shiu University, Taiwan

interaction problems. Recently, Dong and Atluri (2012a) derived a general Trefftz's function suitable for multi-connected region in elasticity that also addressed the hole–hole interactions. Additionally, Dong and Atluri (2012b,c,d, 2013) further combined the micro-model of Voronoi cells to evaluate the macro-mechanical-behavior of heterogeneous material possessing defects, such as voids, inclusions and cracks. Another novel classical approach, based on the alternating iteration among multiple connected regions developed by Kantorovich and Krylov (1964), was also applied among cracks interactions by Han and Atluri (2002), Kuang and Chen (1997), Wang and Atluri (1996).

In the assessment of hole-crack interaction, Hu, Chandra and Huang (1993) modeled unknown Pseudo-tractions pertained on the holes contours, and the cracks were modeled as an unknown distribution of dislocations. This presentation expands alternating iteration to multiple connected holes, and uses the detailed elastic stresses analysis to assess the stress concentrations among ligament between dual interacting holes.

2 Generalized Büeckner's principle

Based on the superposition, Büeckner (1958) derived a very important principle in linear elastic fracture mechanics (LEFM). Since the theory of elasticity is linear, the field in the cracked solid is divided into two parts. One is regular field with no crack which is strained under the same loading conditions as that in the cracked specimen. The other is corrective field that occurs due to the presence of the crack. He expressed that stress intensity factor (SIF) of the cracked solid was completely determined by the corrective field. In the corrective field, crack-faces are loaded by the applied tractions which are equal in magnitude but opposite in sign, and the stress vectors are evaluated along the crack faces as that in un-cracked solid. Fig. 1 illustrates that an infinite plate with a slant crack with aligned angle measured from X-axis is loaded by a remote loadingS^{∞}_{yy}. Since the tractions (boundary stress vectors) along facets of the crack is considered as a continuation of the internal stress distribution. Thereafter this study implements the Mohr's stress transformation and the boundary stress vectors operation, the boundary stress vector on crack in local coordinate (x',y') is shown in Eq. (1). The details are displayed in Fig. 1.

$$\begin{Bmatrix} T_{x'x'} \\ T_{y'y'} \end{Bmatrix}_{upper} = \left(\begin{bmatrix} \cos(\beta) & \sin(\beta) \\ -\sin(\beta) & \cos(\beta) \end{bmatrix} \begin{bmatrix} 0 & 0 \\ 0 & S^{\infty}_{yy} \end{bmatrix} \begin{bmatrix} \cos(\beta) & \sin(\beta) \\ -\sin(\beta) & \cos(\beta) \end{bmatrix}^{\mathrm{T}} \right) \begin{Bmatrix} 0 \\ -1 \end{Bmatrix} = \begin{Bmatrix} -S^{\infty}_{yy}\sin(\beta)\cos(\beta) \\ -S^{\infty}_{yy}\cos^2(\beta) \end{Bmatrix} \tag{1}$$

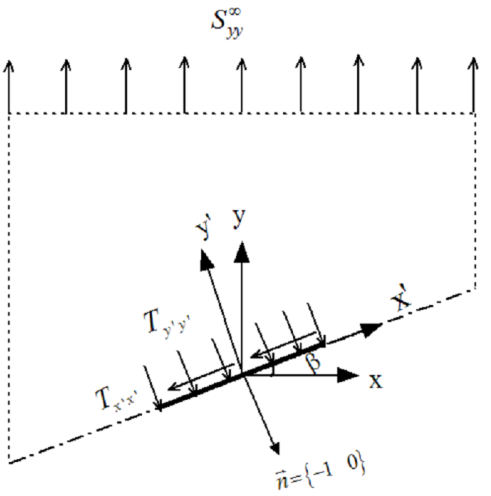

Figure 1: Büeckner's derivated stress vector on the upper crack face

And those for the lower face are

$$\begin{Bmatrix} T_{x'x'} \\ T_{y'y'} \end{Bmatrix}_{lower} = \left(\begin{bmatrix} \cos(\beta) & \sin(\beta) \\ -\sin(\beta) & \cos(\beta) \end{bmatrix} \begin{bmatrix} 0 & 0 \\ 0 & S_{yy}^{\infty} \end{bmatrix} \begin{bmatrix} \cos(\beta) & \sin(\beta) \\ -\sin(\beta) & \cos(\beta) \end{bmatrix}^{\mathrm{T}} \right) \begin{Bmatrix} 0 \\ 1 \end{Bmatrix} = \begin{Bmatrix} S_{yy}^{\infty} \sin(\beta)\cos(\beta) \\ S_{yy}^{\infty} \cos^2(\beta) \end{Bmatrix} \tag{2}$$

However, the tractions on the upper or lower crack faces must be the same in magnitude but opposite in sign for these calculated stress vectors. Rice (1972) extended Büeckner's superposition to use as a fundamental weight function, which the SIF is expressed as a sum of work-like products between applied forces and weight function at their points of application. Kuang and Chen (1997) evaluated plastic envelope around crack tip with the assistance of Büeckner's superposition. After comparing an infinite plate by using conventional crack-tip singular stress solution, they found out that different result aroused.

Fig. 2(a) indicates that the crack is loaded by a pair of symmetric concentrated load p, q on the crack face. And the elastic solution of this problem is regarded as fundamental solution of crack with concentrated loading, which is shown in Eq. (3). The other geometric boundary with concentrated force, for instance, free surface, circular holes or elliptic voids can be also attributed to fundamental solutions. The stress field for crack with concentrated force and SIF are available in the literature.

Eq. (3) displays the stress field and Eq. (4) is SIF of the elastic solution of the problem that is illustrated in Fig. 2(a). The fundamental solution plays a role of weight function. Therefore, the stress solution and SIF solution for the problem denoted in Fig 2(b) can be integrated for the traction distribution ($p(\xi)$, $q(\xi)$) along the crack boundary, as observed in Eq. (5) and Eq. (6).

$$
\begin{aligned}
F_x =& \frac{1}{\pi\rho}\sqrt{\frac{a^2-\xi^2}{r_1 r_2}}\left\{\cos\left(\phi+\frac{\theta_1+\theta_2}{2}\right)\right.\\
&\left.-\frac{y}{\rho}\left[\sin\left(2\phi+\frac{\theta_1+\theta_2}{2}\right)+\frac{r\rho}{r_1 r_2}\sin\left(\phi-\theta+\frac{3(\theta_1+\theta_2)}{2}\right)\right]\right\}
\end{aligned}
$$

$$
\begin{aligned}
G_x =& -\frac{1}{\pi\rho}\sqrt{\frac{a^2-\xi^2}{r_1 r_2}}\left\{2\sin\left(\phi+\frac{\theta_1+\theta_2}{2}\right)\right.\\
&\left.+\frac{y}{\rho}\left[\cos\left(2\phi+\frac{\theta_1+\theta_2}{2}\right)+\frac{r\rho}{r_1 r_2}\cos\left(\phi-\theta+\frac{3(\theta_1+\theta_2)}{2}\right)\right]\right\}
\end{aligned}
$$

$$
\begin{aligned}
F_y =& \frac{1}{\pi\rho}\sqrt{\frac{a^2-\xi^2}{r_1 r_2}}\left\{\cos\left(\phi+\frac{\theta_1+\theta_2}{2}\right)\right.\\
&\left.+\frac{y}{\rho}\left[\sin\left(2\phi+\frac{\theta_1+\theta_2}{2}\right)+\frac{r\rho}{r_1 r_2}\sin\left(\phi-\theta+\frac{3(\theta_1+\theta_2)}{2}\right)\right]\right\}
\end{aligned}
$$

$$
G_y = \frac{y}{\pi\rho^2}\sqrt{\frac{a^2-\xi^2}{r_1 r_2}}\left[\cos\left(2\phi+\frac{\theta_1+\theta_2}{2}\right)+\frac{r\rho}{r_1 r_2}\cos\left(\phi-\theta+\frac{3(\theta_1+\theta_2)}{2}\right)\right] \tag{3}
$$

$$
F_{xy} = \frac{y}{\pi\rho^2}\sqrt{\frac{a^2-\xi^2}{r_1 r_2}}\left[\cos\left(2\phi+\frac{\theta_1+\theta_2}{2}\right)-\frac{r\rho}{r_1 r_2}\cos\left(\phi-\theta+\frac{3(\theta_1+\theta_2)}{2}\right)\right]
$$

$$
\begin{aligned}
G_{xy} =& \frac{1}{\pi\rho}\sqrt{\frac{a^2-\xi^2}{r_1 r_2}}\left\{\cos\left(\phi+\frac{\theta_1+\theta_2}{2}\right)\right.\\
&\left.-\frac{y}{\rho}\left[\sin\left(2\phi+\frac{\theta_1+\theta_2}{2}\right)+\frac{r\rho}{r_1 r_2}\cos\left(\phi-\theta+\frac{3(\theta_1+\theta_2)}{2}\right)\right]\right\}
\end{aligned}
$$

$$
\left\{\begin{array}{c} K_I \\ K_{II} \end{array}\right\}_{\pm a} = \frac{1}{\sqrt{\pi a}}\left\{\begin{array}{c} p(\xi) \\ q(\xi) \end{array}\right\}\sqrt{\frac{a\pm\xi}{a\mp\xi}}d\xi \tag{4}
$$

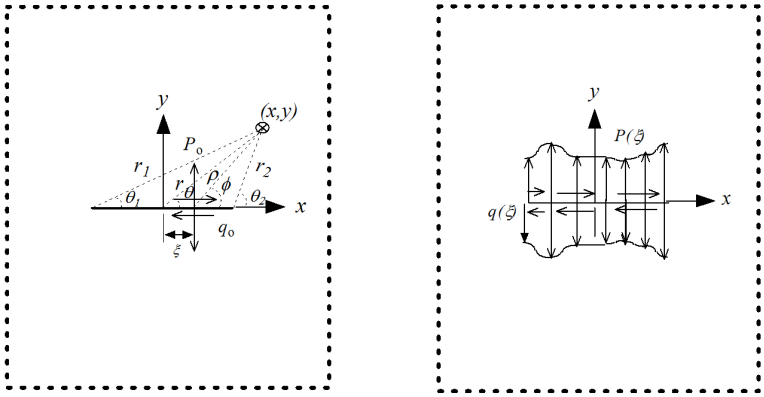

Figure 2: Schematic drawing of a crack with (a) a concentrated load (b) distributed traction

$$\begin{aligned}
\sigma_{xx}^{c} &= pF_x(a,r_1,r_1,\rho,\theta_1,\theta_2,\phi,\xi) + qG_x(a,r_1,r_1,\rho,\theta_1,\theta_2,\phi,\xi) \\
\sigma_{yy}^{c} &= pF_y(a,r_1,r_1,\rho,\theta_1,\theta_2,\phi,\xi) + qG_y(a,r_1,r_1,\rho,\theta_1,\theta_2,\phi,\xi) \\
\tau_{xy}^{c} &= pF_{xy}(a,r_1,r_1,\rho,\theta_1,\theta_2,\phi,\xi) + qG_{xy}(a,r_1,r_1,\rho,\theta_1,\theta_2,\phi,\xi)
\end{aligned} \tag{5}$$

$$\begin{cases}
\sigma_{xx} = \int_{-a}^{a} [p(\xi)F_x + q(\xi)G_x]\,d\xi \\
\sigma_{yy} = \int_{-a}^{a} [p(\xi)F_y + q(\xi)G_y]\,d\xi \\
\tau_{xy} = \int_{-a}^{a} [p(\xi)F_{xy} + q(\xi)G_{xy}]\,d\xi
\end{cases} \tag{6}$$

3 Fundamental solution

3.1 Perforated plate with concentrated load on its circular hole edge

The fundamental solution of a hole problem in an infinite plate subjected to a point force of components p_x and $p_y$acts at a point on its circular boundary, say, $(R_o,0)$ where $R_o$is the radius of the hole as denoted in Fig. 3. Dundurs and Hetenyi (1961), Hetenyi and Dundurs(1962) evaluated stresses evolution at any position (x,y) on the plate that is demonstrated in Eq. (7) and (8) where κ=*3-*ν is for plane strain , and κ=*(1-*ν*)/(1-2*ν) is for plane stress.

$$\sigma_{ij}^{P_k} = \frac{1}{2\pi(1+\kappa)} H_{ijk}(x,y;R_o)\,P_k \quad i,j,k = x,y \tag{7}$$

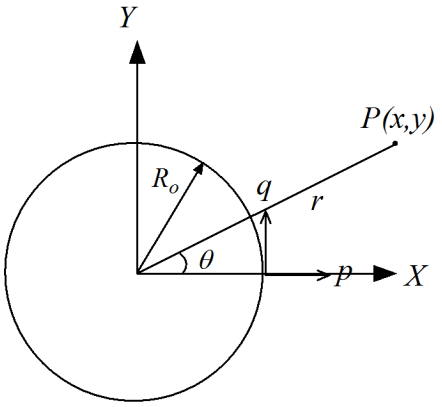

Figure 3: Circular hole with a concentrated load on its edge

$$H_{xxx}(x,y;R_o) = \frac{2(1+\kappa)x^3}{r_0^4} - \frac{4(1+\kappa)x_1^3}{r_1^4} - R_o(1+\kappa)\left(-\frac{1}{r_0^2}+\frac{2x^2}{r_0^4}\right) + {R_o}^2\kappa\left(\frac{6x}{r_0^4}-\frac{8x^3}{r_0^6}\right)+(-1+\kappa)\left(-\frac{x}{r_0^2}+\frac{2x^3}{r_0^4}\right),$$

$$H_{xyx}(x,y;R_o) = -\frac{2R_o(1+\kappa)xy}{r_0^4}+\frac{2(1+\kappa)x^2y}{r_0^4}-\frac{4(1+\kappa)x_1^2y}{r_1^4} + {R_o}^2\kappa\left(\frac{2y}{r_0^4}-\frac{8x^2y}{r_0^6}\right)+(-1+\kappa)\left(-\frac{y}{r_0^2}+\frac{2x^2y}{r_0^4}\right),$$

$$H_{yyx}(x,y;R_o) = -R_o(1+\kappa)\left(\frac{1}{r_0^2}-\frac{2x^2}{r_0^4}\right)+{R_o}^2\kappa\left(-\frac{6x}{r_0^4}+\frac{8x^3}{r_0^6}\right) + (1+\kappa)\left(\frac{2x}{r_0^2}-\frac{2x^3}{r_0^4}\right)+(-1+\kappa)\left(\frac{3x}{r_0^2}-\frac{2x^3}{r_0^4}\right) - 2(1+\kappa)\left(\frac{2x_1}{r_1^2}-\frac{2x^3}{r_1^4}\right),$$

$$H_{xxy}(x,y;R_o) = -\frac{2R_o(1+\kappa)xy}{r_0^4}+\frac{2(1+\kappa)x^2y}{r_0^4}-\frac{4(1+\kappa)x_1^2y}{r_1^4} + {R_o}^2\kappa\left(\frac{2y}{r_0^4}-\frac{8x^2y}{r_0^6}\right)+(-1+\kappa)\left(\frac{y}{r_0^2}+\frac{2x^2y}{r_0^4}\right),$$

$$
\begin{aligned}
H_{xyy}(x,y;R_o) &= R_o(1+\kappa)\left(-\frac{1}{r_0^2}+\frac{2x^2}{r_0^4}\right)+{R_o}^2\kappa\left(-\frac{6x}{r_0^4}+\frac{8x^3}{r_0^6}\right)\\
&\quad+(-1+\kappa)\left(\frac{x}{r_0^2}-\frac{2x^3}{r_0^4}\right)-(1+\kappa)\left(-\frac{2x}{r_0^2}+\frac{2x^3}{r_0^4}\right)\\
&\quad+2(1+\kappa)\left(-\frac{2x_1}{r_1^2}+\frac{2x_1^3}{r_1^4}\right),\\
H_{yyy}(x,y;R_o) &= \frac{2R_o(1+\kappa)xy}{r_0^4}+{R_o}^2\kappa\left(-\frac{2y}{r_0^4}+\frac{8x^2y}{r_0^6}\right)+(-1+\kappa)\left(\frac{y}{r_0^2}-\frac{2x^2y}{r_0^4}\right)\\
&\quad-(1+\kappa)\left[\left(-\frac{2y}{r_0^2}\right)+\left(\frac{2x^2y}{r_0^4}\right)\right]+2(1+\kappa)\left(-\frac{2y}{r_1^2}+\frac{2x_1^2y}{r_1^4}\right),\\
&\text{where}\qquad x_1=(x-R_o),\ r_0^2=\left(x^2+y^2\right),\ \text{and}\ r_1^2=\left(x_1^2+y^2\right)
\end{aligned}
\tag{8}
$$

Like the treaties in crack problem, the solution of point loaded hole, as denoted in Eq. (7), can be integrated around the circular boundary to represent a situation that the hole is under distributed pressure.

3.2 Solutions comparison for a perforated plate with remote axial loading

A test problem was intended for the application of the generalized Bückner's superposition. Fig. 4 indicates that Büeckner's superposition is applied on a perforated plate with remote tractionσ^∞. This problem is well-defined in every textbook on elasticity and this presentation selects this problem as an example of assessing the numerical integration conformance and limitation. Therefore, the tractions evolved on circular contour as observed in Fig. 4(c) can be easily implanted as

$$
\begin{aligned}
p(\theta) &= \sigma^\infty\cos^2(\theta)\\
q(\theta) &= \sigma^\infty\sin(\theta)\cos(\theta)
\end{aligned}
\tag{9}
$$

The whole field stress distribution in Fig. 4(a) can be evaluated by the superposition of stress field in Fig. 4(b) and Fig. 4(c) respectively. Stress field in Fig. 4(b) can be simply expected as that in Eq. (3).

$$
\begin{bmatrix} \sigma_{xx} & \tau_{xy} \\ \tau_{xy} & \sigma_{yy} \end{bmatrix} = \begin{bmatrix} 0 & 0 \\ 0 & \sigma^\infty \end{bmatrix}
\tag{10}
$$

For the problem of Fig 4(c), Eq. (7, 8) can be evolved and then integrated along the circular contour. This study is dedicated to numerical integration which Gauss-Legendre quadrature is implanted in the calculation due to its feasibility in non-linear assessment. Fig. 5 shows that the radial distance is chosen for $r/R_0 = 1.1$

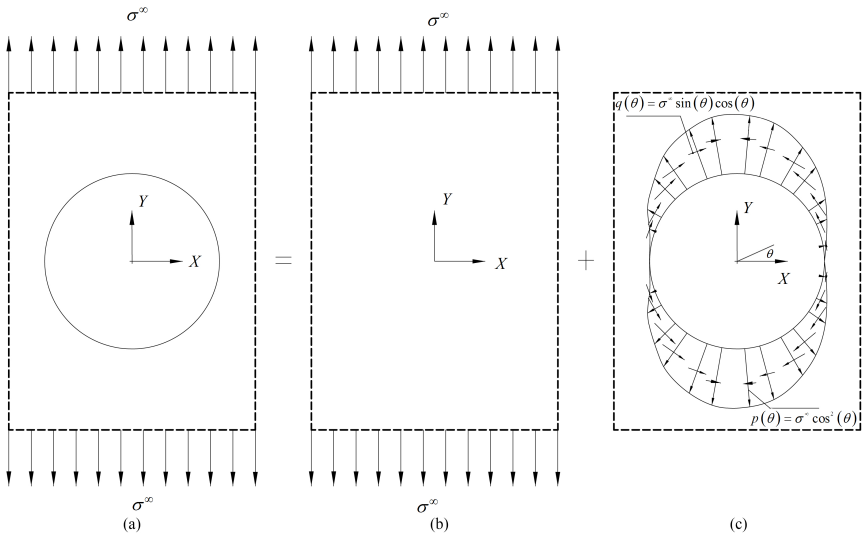

Figure 4: Büeckner's superposition of a perforated plate with remote tractions

and $\theta = 0^0 \rightarrow 360^0$, Gaussian integration points are selected 500, 1500 and 3000 respectively. The outcome indicates that good conformance compares to the analytical solution of shear stress and hoop stress, but some deviation is occurred on radial stress. However higher selected Gaussian points can achieve better agreement of radial stress estimation, yet the computation time is increased. This presentation checks on the conventional defined stress concentration location, i.e., at the site of θ=0^o and θ=180^o for hoop stress and finds out that even low chosen Gaussian points can result in good accuracy of $2.5\sigma^{\infty}$. When calculation is taken at the site of its own, then Eq. (8) is unbound. However when calculation is made on the circular contour, the tractions evolved at the site of its own remain $p(\theta)$, $q(\theta)$ only. The whole tractions on this site shall be superposed by its own $p(\theta)$, $q(\theta)$ and the induced tractions from loading are at other sites.

4 Dual holes interactions

In the evaluation of dual holes interactions, Schwartz-Neuman alternating iteration is employed to solve the interactions between holes. Alternating technique reduces problem originally in multi-connected regions to a sequence of simply connected domain problems. Successively iterative superposition would be therefore engaged to achieve a satisfactorily solution common to each domain. The convergence of the alternating algorithm for Neuman boundary value problem of doubly connected re-

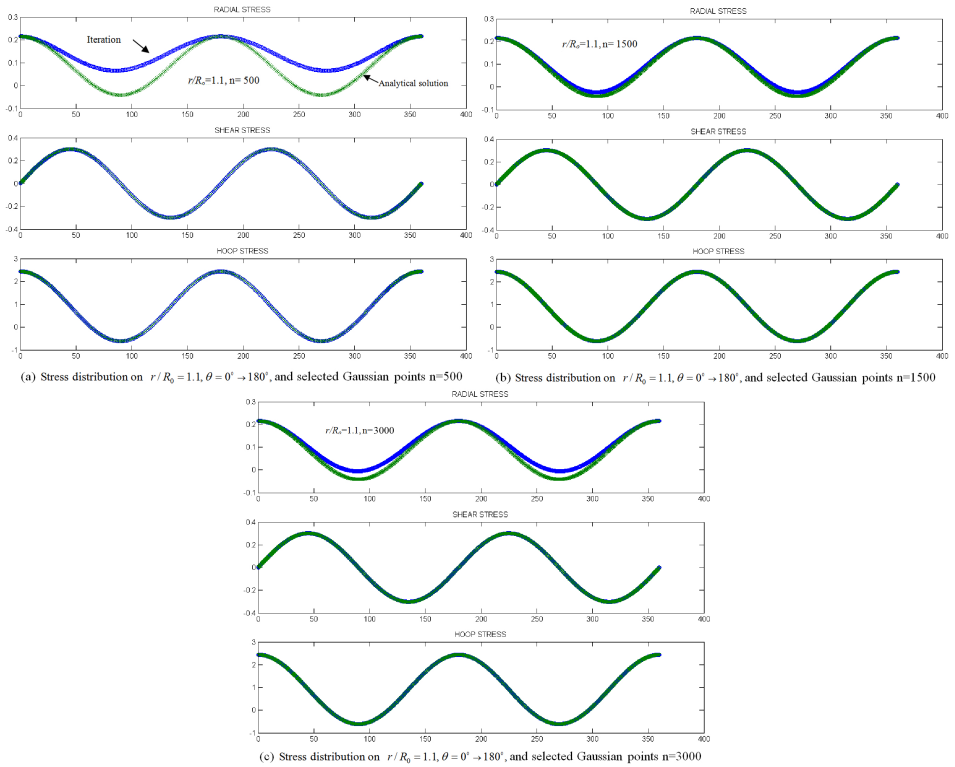

Figure 5: Radial, shear and hoop stress distribution on $r/R_0 = 1.1,\ \theta = 0^0 \to 180^0$, for varying selected Gaussian points (a) n=500 (b) n=1500 and (c) n=3000

gion had been proven in Sokolnikoff's (1956) monograph. The alternating method combined with the analytical solution in simply connected domain, and then elaborated numerical computations in a series of successive iterations.

As denoted in the Schwarz's alternating iteration algorithm, fundamental analytic solution is required for each simply connected region respectively. For the interacting problem of dual holes, as illustrated in Fig.6(a), Büeckner's superposition is employed again, and this multi-connected problem is broken down into two subproblems as illustrated in Fig. 6(b, c). Initial traction components (p_2^0, q_2^0, p_3^0 and q_3^0) on the hole edge are displayed in Eq. (11).

$$\begin{array}{llll} p_2^0(\theta_2) = \sigma^\infty \cos^2(\theta_2) & , q_2^0(\theta_2) = \sigma^\infty \sin(\theta_2)\cos(\theta_2) & \text{for hole2} \\ p_3^0(\theta_3) = \sigma^\infty \cos^2(\theta_3) & , q_2^0(\theta_3) = \sigma^\infty \sin(\theta_3)\cos(\theta_3) & \text{for hole3} \end{array} \tag{11}$$

Fig. 6(c) can be further isolated as denoted in Fig. 7, in which these two sub-

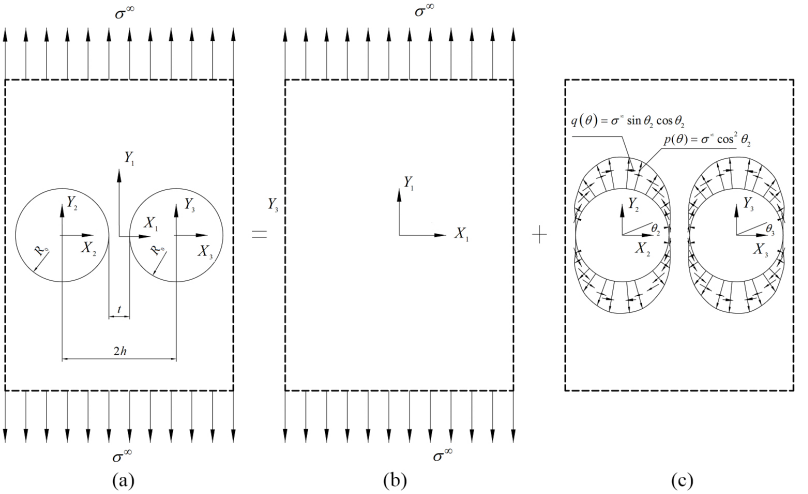

Figure 6: Büeckner's superposition for an infinite plate contains two interacting holes

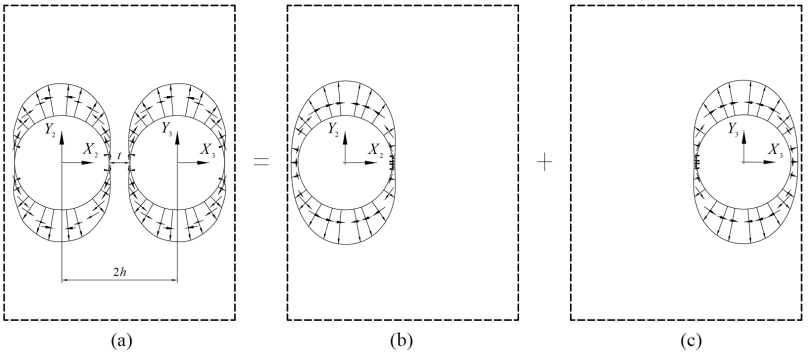

Figure 7: Isolation of two interacting holes by use of successive alternating iteration

problems of Fig. 7(b) and (c) are considered as simple-connected region with unknown tractions on its boundaries respectively. After successive iteration to gradually nullify the boundary tractions on the holes of Fig. 7(a), the interacting two holes are isolated. The artificial super-imposed traction to nullify the existing tractions on the holes edges shall be collected. After the iterating stops, i.e., the absolute normalized induced tractions on both holes generated by the other hole are less than 10^{-6} in the numerical assessment; nullification on both holes contours is thus achieved. The collected artificial tractions are then adjoined to represent the tractions on the holes edge in the isolations, as depicted in Fig. 7(b) and (c). Therefore, the stress concentration factors at both near site ($\theta_2 = 0^\circ,\ \theta_3 = 180^\circ$) and far site ($\theta_3 = 0^\circ,\ \theta_2 = 180^\circ$) are thus determined.

Table 1: Stress concentrations of dual holes interaction with varying pitches

Pitch (t/R_o)	Gaussian points	Near site	Far site	Iteration number
9	50	2.9970	3.0043	3
7	50	2.9949	3.0085	3
5	50	2.9922	3.0201	4
3	50	3.0202	3.0660	5
2	50	3.2641	3.1510	7
1.8	50	3.4425	3.1846	9
1.6	50	3.7684	3.2306	10
1.4	50	4.4227	3.2977	14
1.2	50	6.1114	3.4104	26
1.2	100	6.1060	3.4104	27
1.1	50	8.5261	3.5073	92
1.1	100	8.6910	3.5120	54
1.1	500	8.6885	3.5120	54
1.1	1000	8.6885	3.5120	54

Attention must be paid, as Eq. (7) is unbound when calculation is made at the site of its own. When calculation is completed at sites along the circular contour, the tractions involved at the site of its own $p(\theta)$, $q(\theta)$ can be singular, and the tractions on this very site can be assessed as $p(\theta)$, $q(\theta)$ only. The whole tractions on this site are regarded as a whole by its own $p(\theta)$, $q(\theta)$ and by the induced tractions strained by other sites along the contour.

The stress concentration for dual holes interaction is shown in Table 1 for different pitches between holes. Because of the accurate stresses estimation in this numerical scheme, the dual holes are located in close proximity and highly nonlinear assess-

Table 2: Stress concentrations of dual holes interaction with close proximity

Pitch (t/R_o)	Gaussian points	Near site	Far site	Iteration number
1.08	500	9.7654	3.5414	68
1.08	800	9.7654	3.5414	68
1.06	500	11.3668	3.5768	93
1.04	500	14.0954	3.6216	147
1.02	500	20.3520	3.6854	335
1.02	1000	20.3622	3.6854	319
1.01	500	-	-	30,000%
1.01	1000	29.3160	3.7345	820

% no convergence

ment would be manipulated in Gaussian-Legendre quadrature, as shown in Table 2. However the convergence is good enough as shown in Table 1, despite the case of t/R_o=1.01. A large quantity of Gaussian points must be selected to adjust the highly non-linear developed stress. The stress concentration factors of the main hole (originally is 3 for far distant pitch between holes) are disturbed by the other approaching hole. The outcome is evident that stress concentration is altered when t/R_o <3, for closer proximity the stronger of the concentration. The near site is always enhanced much more than far site for t/R_o <3. But for the pitch t/R_o >3, far site is enhanced slightly and near site is shielded a little bit. In the case of t/R_o >3, a particular phenomena take place that stress concentration at far site gradually increases to a little bit far from 3; however, near site comes in a opposite way. Under such situation, only slight disturbance and deviation take place from the distinctive stress concentration factor of 3.

5 Conclusions

1. Büeckner's superposition and alternating iteration methods are applicable for dual holes interaction analysis, even crack is not prevailed in the problem.

2. The whole field stress distribution is accurately estimated for dual holes interaction, even in a very close proximity of these dual holes. However, the above mentioned methods must be employed in the Gaussian-Legendre quadrature evaluation to confirm the whole field stress assessment to be precise, and larger Gaussian points must be selected to revise the enormous non-linearity developed in the stress evaluation.

3. A particular phenomena take place that stress concentration at far site grad-

ually increases to a little bit far from 3, as the pitch $t/R_o > 3$, but near site comes in a opposite way.

References:

Buckner, H. F. (1958): The propagation of cracks and the energy of elastic deformation. *ASME J. Appl. Mech.*, vol. 80, pp. 1225–1230.

Dong, L.; Atluri, S. N. (2012a): A simple multi-source-point Trefftz method for solving direct/inverse SHM problems of plane elasticity in arbitrary multiply-connected domains. *CMES*, vol. 85, no.1, pp.1-43

Dong, L.; Atluri, S.N. (2012b): Development of 3D T-Trefftz Voronoi cell finite elements with/without spherical voids &/or elastic/rigid inclusions for micromechanical modeling of heterogeneous materials. *CMC: Computers Materials and Continua*, vol. 29, no.1, pp. 169-211.

Dong, L.; Atluri, S.N. (2012c):Development of 3D Trefftz Voronoi cells with ellipsoidal voids &/or elastic/rigid inclusions for micromechanical modeling of heterogeneous materials. *CMC: Computers Materials and Continua*, vol.1, pp. 39-81.

Dong, L.; Atluri,S.N (2013): SGBEM Voronoi cells (SVCs), with embedded arbitrary-shaped inclusions, voids, and/or cracks for micromechanical modeling of heterogeneous materials. *CMC: Computers Materials and Continua,* vol. 33, no.1, pp. 111-154.

Dundurs, J.; Hetenyi, M. (1961): The elastic plane with a circular insert loaded by a radical force. *Journal of Applied Mechanics*, vol. 28, pp.103-111.

Han, Z.D.; Atluri, S.N. (2002): SGBEM (for cracked local subdomain) - FEM (for uncracked global structure) alternating method for analyzing 3D surface cracks and their fatigue-growth. *CMES-Computer Modeling in Engineering & Sciences*, vol. 3, no. 6, pp. 699-716.

Hetenyi, M.; Dundurs, J. (1962): The elastic plane with a circular insert loaded by a tangentially direct force. *Journal of Applied Mechanics*, vol. 28, pp.277-291.

Horii, H.; Nemat-Nasser, S. (1985): Elastic fields of interacting inhomogeneities. *Int. J. Solids Struct.,* vol. 21, pp. 731–745.

Hu, K.X.; Chandra, A.; Huang, Y. (1993): Multiple void-crack interaction. *Int. J. Solids Struct.*, vol. 30, no. 11, pp. 1473–1489 .

Inglish, C. E. (1913): Stress in a plate due to the presence of cracks and sharp corners. *Transactions of the Institute of Naval Architects*, pp. 219-230.

Kantorrovich L. V.; Krylov, V. I. (1964): *Approximate Methods of Higher Analysis.* Interscience, New York.

Kuang J. H.; Chen C. K. (1997): Crack tip plastic zones estimation using Büeck-

nerip plastic zones. *International Journal of Fracture*, vol. 88, L39-L44.

Kuang J. H.; Chen C. K. (1998): Equivalence for two interacting parallel cracks. *ASME, Journal of Pressure Vessel Technology,* vol. 120, 424-430.

Mushelishvili, N. I. (1953): Some Basic Problems of the Mathematical Theory of Elasticity. Noordhoff, Groningen-Holland.

Nisitani, H.; Chen, D. H. (1997): Body force method and its application to numerical and theoretical problems in fracture and damage. *Computational Mechanics*, vol. 19, pp. 470-480.

Rice, J. R. (1972): Some Remarks on elastic crack-tip stress fields. *Int. J. Solids Structures*, vol. 8, pp. 751-758.

Savin, G. N. (1961): *Stress Concentrations Around Holes*. Pergamon Press, London.

Sokolnikoff. I. S. (1956): *Mathematical Theory of Elasticity*. 2^{nd} ed. MacGraw-Hill, New York.

Wang, L; Atluri S. N. (1996): Recent advances in the alternating method for elastic and inelastic fracture analyses. *Computer Methods in Applied Mechanics and Engineering*, vol. 137, pp1-58.